IL NUOVO CIMENTO Vol. 27 C, N. 5 Settembre-Ottobre 2004
DOI 10.1393/ncc/i2005-10026-4

Negative refraction in crystals with spatial dispersion

L. Silvestri([1]), O. A. Dubovski([2]), G. C. La Rocca([1]), F. Bassani([1]) and V. M. Agranovich([2])([3])

([1]) *Scuola Normale Superiore - Pisa, Italy*
([2]) *Institute of Spectroscopy, Russian Academy of Sciences Troitsk, Moscow obl. 142190, Russia*
([3]) *UTD-NanoTech Institute, The University of Texas at Dallas Richardson, Texas 75083-0688, USA*

(ricevuto il 20 Gennaio 2005)

Summary. — We predict, on the basis of numerical simulations, that organic crystals with appropriate spatial dispersion can exhibit negative refraction at optical frequencies near excitonic transitions. In particular we demonstrate that a plane slab of such materials is able to focus light coming from an oscillating point dipole. The intensity of the resulting image and its sharpness are mainly limited by absorption but its very presence unambiguously demonstrates negative refraction at the slab/vacuum interface. In our approach the medium is characterized by a generalized dielectric constant and all the relevant fields are computed by solving Maxwell equations with appropriate boundary conditions.

PACS 78.20.Ci – Optical constants (including refractive index, complex dielectric constant, absorption, reflection and transmission coefficients, emissivity).
PACS 42.25.Bs – Wave propagation, transmission and absorption.

1. – Introduction

It is well known that the propagation of electromagnetic waves in an isotropic material with a negative dielectric permittivity $\epsilon(\omega) < 0$ and a negative magnetic permeability $\mu(\omega) < 0$ can exhibit very unusual properties [1]. In such media for instance the wave vector $\mathbf{k}$, the electric field $\mathbf{E}$ and the magnetic field $\mathbf{H}$ form a left-handed orthogonal set, that is why they are usually termed Left Handed Materials (LHM) in contrast to the ordinary Right Handed Materials (RHM).

The most foundamental property of wave propagation in LHM is that the group velocity $\mathbf{v}_{\mathrm{gr}}$ is opposite to the wave vector $\mathbf{k}$, or in other words that the group velocity is negative. From that property it follows that also the Poynting vector is opposite to $\mathbf{k}$, and a further consequence is the negative refraction at a LHM/RHM interface, which is required by causality [2].

Due to their unique behavior LHM are recently attracting a lot of interest, both from the theoretical and the experimental point of view [3-20], specially for their potential applications in building superlenses, *i.e.* lenses with a resolution beyond the diffraction limit [5-7, 16]. At present LHM have been created that are effective in the microwave region of the spectrum [4, 9, 10], but much more attention is now directed to the design of structures working at optical frequencies. It has been proposed that photonic-gap materials can behave as LHM at such frequencies and numerical simulations, together with the first experiments, seem to confirm this hypothesis [11-16].

The "left-handed" behavior of a material is usually associated to the condition $\epsilon(\omega) < 0$, $\mu(\omega) < 0$, but, as we already mentioned, all the main properties of a LHM can be derived from the assumption that the group velocity is negative. This latter condition can be more general than the former, as discussed by Agranovich and coworkers [21]. In particular they showed that if spatial dispersion is taken into account, it is possible to have a negative group velocity even for $\mu = 1$. This is of fundamental importance at optical frequencies, since the magnetic permeability has no real meaning and it can be always assumed that $\mu = 1$ [22].

In this paper we will show that in molecular crystals possessing a specific spatial dispersion it is possible to have additional waves with a negative group velocity for frequencies near the excitonic resonances. We will also present the result of numerical simulations demonstrating that such class of materials can behave as LHM under appropriate conditions. In particular we prove that an infinite plane slab of such materials is able to focus light coming from an oscillating point dipole, as schematically shown in fig. 1.

The paper is organized as follows. In sect. **2** we present the theoretical approach, which consists in characterizing a medium response completely by a generalized electric polarization, and write an expression for the effective dielectric permittivity near an excitonic resonance. In sect. **3** we discuss the problem of the boundary conditions for a plane wave of a single frequency in the presence of an infinite slab characterized by the effective dielectric constant described in sect. **2**. In sect. **4** we describe the details of the numerical simulation and present the results. Conclusions are presented in sect. **5**.

2. – The generalized dielectric constant

When describing the behavior of LHM, it is customary to use the set of fields $\mathbf{E}$, $\mathbf{D}$, $\mathbf{B}$ and $\mathbf{H}$, with $\mathbf{D} = \epsilon(\omega)\mathbf{E}$ and $\mathbf{H} = \mu(\omega)\mathbf{B}$ for monochromatic waves. A more general approach [21], which is more suitable at optical frequencies, is to consider the set of fields $\mathbf{E}$, $\mathbf{D}$, $\mathbf{B}$, with $\mathbf{D} = \tilde{\epsilon}(\omega, \mathbf{k})\mathbf{E}$ and $\mathbf{B} = \mathbf{H}$. This set of fields satisfies the macroscopic Maxwell equations

$$\nabla \times \mathbf{B} = \frac{1}{c}\frac{\partial \mathbf{D}}{\partial t}, \tag{1}$$

$$\nabla \times \mathbf{E} = -\frac{1}{c}\frac{\partial \mathbf{B}}{\partial t}, \tag{2}$$

$$\nabla \cdot \mathbf{B} = 0, \quad \nabla \cdot \mathbf{D} = 0, \tag{3}$$

while the linear optical response of the medium is completely determined by the generalized dielectric tensor $\tilde{\epsilon}(\omega, \mathbf{k})$. The main reason for adopting such a method is that spatial

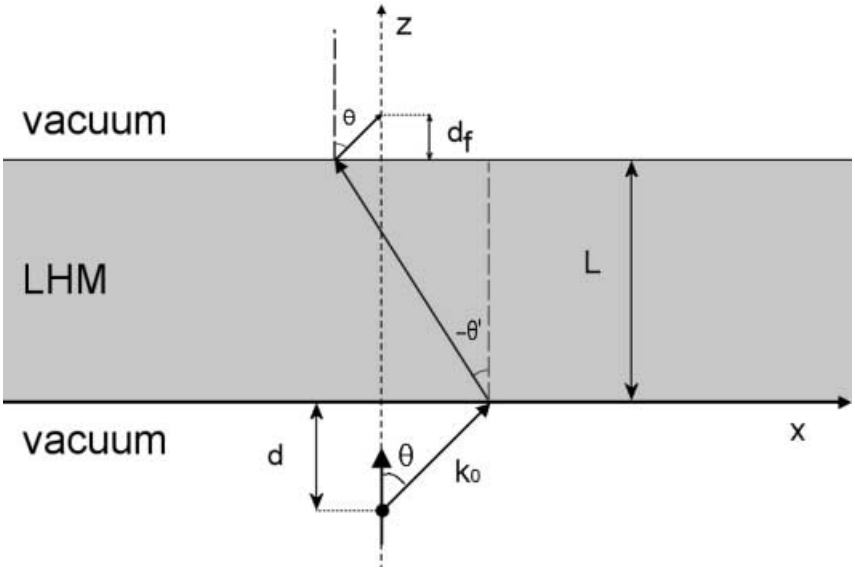

Fig. 1. – Light coming from a source dipole can be focused by a left-handed slab, due to negative refraction at the LHM/vacuum interface. The dipole is placed at a distance d from the slab surface and a real image is formed at a distance d_f from the opposite surface of the slab.

dispersion can be easily taken into account, while keeping the calculations simple in the case of a nonmagnetic material. Of course the method is completely general and retains its validity also when applied to magnetic materials. In the well-studied case $\epsilon(\omega) < 0$ and $\mu(\omega) < 0$, for instance, this has been shown by Agranovich and coworkers [21], who proved that all the properties connected to the negative group velocity can be correctly

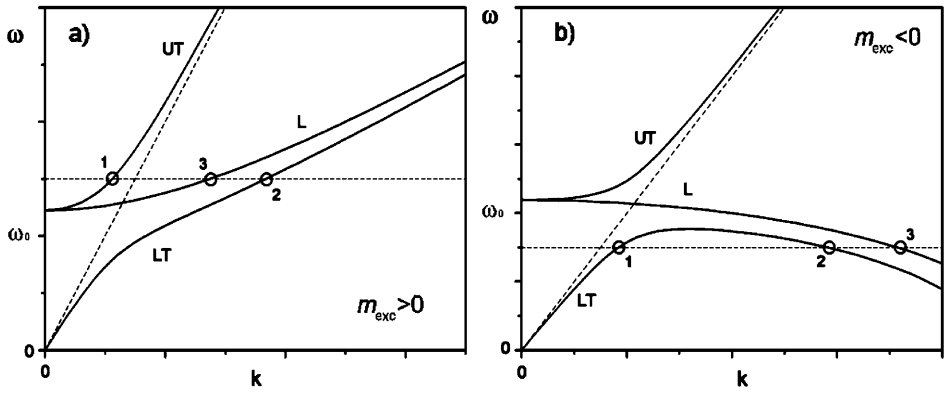

Fig. 2. – Dispersion curves for an organic crystal, near an excitonic resonance when the exciton mass is positive (a) or negative (b). Three branches are present: an Upper Transverse (UT), a Lower Transverse (LT) and a Longitudinal (L) polariton. At some frequencies above (below) the excitonic transition frequency ω_0 three modes are allowed to propagate inside the crystal when the excitonic mass is positive (negative).

described by the E, D, B approach. Moreover they noticed that, if spatial dispersion is taken into account, a negative group velocity can be also obtained in nonmagnetic materials as we will show below for molecular crystals.

In this work we consider in detail the case of an isotropic nonmagnetic material with spatial dispersion. In such a medium the dielectric tensor reduces to a scalar which, near an isolated excitonic resonance, can be written in the form [2]

$$\tilde{\epsilon}(\omega, \mathbf{k}) = \epsilon_{\mathrm{b}} + \frac{F}{\omega_0^2 - \omega^2 - i\gamma\omega + \alpha k^2}\,. \tag{4}$$

In the above expression ω_0, F and $\gamma > 0$ are the frequency, oscillator strength and half width of the excitonic resonance, respectively, ϵ_{b} is a background dielectric constant that includes the contribution of all the other resonances at different frequencies, and

$$\alpha = \frac{\hbar\omega_0}{m_{\mathrm{exc}}}\,, \tag{5}$$

m_{exc} being the exciton effective mass. The inclusion of spatial dispersion, through the wave vector dependence of the excitonic transition in expression (4), leads to the appearance of additional exciton-polariton waves. The dispersion law for transverse waves can be found from the equation

$$\tilde{\epsilon}(\omega, \mathbf{k}) = \frac{k^2 c^2}{\omega^2}\,, \tag{6}$$

which has in general two solutions, an Upper Transverse polariton branch $\omega_{\mathrm{UT}}(\mathbf{k})$, and a Lower Transverse polariton branch $\omega_{\mathrm{LT}}(\mathbf{k})$. In our analysis we will also include longitudinal waves, whose dispersion $\omega_{\mathrm{lo}}(\mathbf{k})$ is derived from the equation

$$\tilde{\epsilon}(\omega, \mathbf{k}) = 0. \tag{7}$$

The main features of the dispersion curves depend on the sign of m_{exc}, as schematically shown in fig. 2. It can be seen that for some range of frequencies two transverse polariton modes are allowed, which have been denoted in the figure by the numbers 1 and 2. It is also evident from the figures that the additional transverse waves, denoted by the number 2, and the longitudinal waves, denoted by 3, have a positive group velocity $v_{\mathrm{gr}} = \partial\omega/\partial k$ for $m_{\mathrm{exc}} > 0$ and a negative group velocity for $m_{\mathrm{exc}} < 0$.

The existence of additional waves has been demonstrated in many crystals, the most convincing experiments having being conducted in semiconductors near the Wannier-Mott exciton resonances [2]. However the effective mass of Wannier-Mott excitons is usually positive, leading to an additional exciton-polariton wave with a positive group velocity. In organic crystals instead Frenkel excitons can have both positive or negative effective masses. This is due to the fact that they have a small radius and that the resonant intermolecular interaction strongly depends on molecular orientation, leading to different signs of m_{exc} in different directions.

Since we are interested in investigating the possibility to obtain a negative refraction in such organic crystals, we will consider in the following an isotropic material with the generalized dielectric function (4) and $\alpha < 0$, meaning that the exciton effective mass is assumed isotropic and negative. We believe that such approach will allow us to clarify the role of additional waves with negative group velocity in such materials, without

complicating too much the calculations. We also believe that the use of powders could provide an isotropic material with the desired properties. A more detailed investigation, considering crystals with uniaxial symmetry and an anisotropic excitonic effective mass will be performed in the future.

We now briefly discuss some properties of the optical constants. It is useful to define the refractive index, which, at a given frequency ω, is defined as

$$n^2(\omega) = \frac{k^2(\omega)c^2}{\omega^2}\,, \tag{8}$$

and it is of course different for each of the three waves that can propagate inside our material. We believe that the sign of n has no real meaning since neither Maxwell's equations nor the boundary conditions include odd powers of the refractive index, that is why we will always use n^2, in order to avoid complications in the definition of n.

Some meaningful relations can be instead derived for the real and imaginary parts of the optical constants. In an isotropic medium the complex wave vector of a plane wave can be written as

$$\mathbf{k} = (k' + ik'')\hat{\mathbf{k}}\,. \tag{9}$$

The wave intensity must decay exponentially in the direction of the energy propagation, which in the case of a nearly lossless material is the direction of the Poynting vector, *i.e.* $\hat{\mathbf{k}}$ for a RHM, and $-\hat{\mathbf{k}}$ for a LHM. It follows then from eq. (8) that

$$\begin{cases} n'n'' > 0 & \text{for a RHM}\,, \\ n'n'' < 0 & \text{for a LHM}\,, \end{cases} \tag{10}$$

where we write $n = n' + in''$. The above relations hold for an isotropic nearly lossless material and are independent of the sign of the refractive index n.

3. – Focusing light with a LH slab

We consider the problem of an oscillating point dipole placed in vacuum at a distance d from an infinite plane slab of thickness L and with its dipole moment perpendicular to the slab. Our goal is to prove that if the generalized dielectric constant of the slab is given by expression (4) with $\alpha < 0$, then light is focused on the opposite side of the slab and a real image of the dipole is formed. For the sake of clarity we will assume the dipole located at $(0, 0, z_0)$ and the slab delimited by the two planes $z = 0$ and $z = L$, so that the dipole moment is directed along the z-axis, as shown in fig. 1.

In order to have an image behind the slab, it is necessary to have negative refraction at the interface between our material and the vacuum. As already discussed, in the case of a negative exciton mass we see from fig. 2b that, choosing an appropriate oscillating frequency below the excitonic resonance ω_0, we can have inside the slab two propagating waves with a negative group velocity: one transverse mode with dispersion $\omega_{\mathrm{LT}}(\mathbf{k})$, denoted by the number 2 in the figure, and a longitudinal mode with dispersion $\omega_{\mathrm{lo}}(\mathbf{k})$, denoted by the number 3.

In the following we will always assume to be in the range of parameters and of frequencies for which dispersion is described by fig. 2b. Therefore inside the slab we will always have one transverse normal mode, one transverse additional mode, and one longitudinal mode, that will be denoted by the superscripts (1), (2) and (3), respectively, as

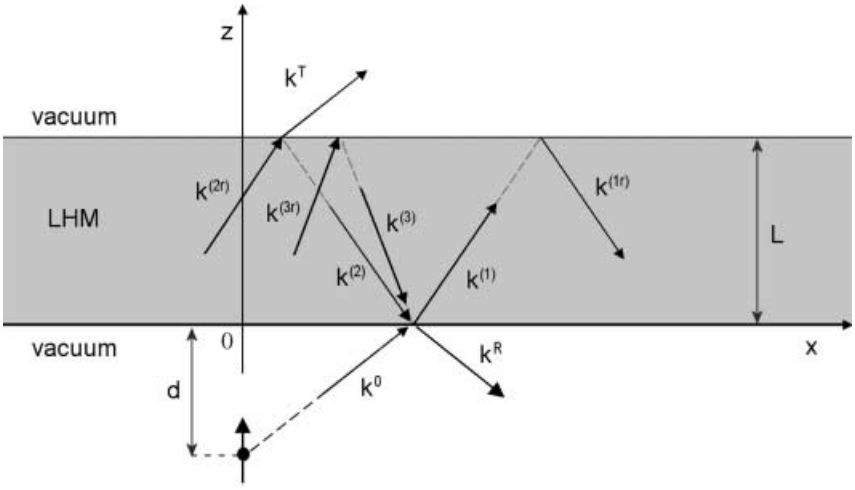

Fig. 3. – Wave vectors of all the plane waves that propagate when an incident plane wave of single frequency is considered.

in the figure. The corresponding wave vectors will be denoted by $\mathbf{k}^{(1)}$, $\mathbf{k}^{(2)}$, $\mathbf{k}^{(3)}$ if they are propagating toward positive z direction and $\mathbf{k}^{(1r)}$, $\mathbf{k}^{(2r)}$, $\mathbf{k}^{(3r)}$ otherwise. In fig. 3 we show the wave vectors of all the relevant waves propagating in vacuum and in the slab for the case of an incident plane wave of a single frequency with wave vector $\mathbf{k}^0$. We stress again that inside the slab the waves propagating away from the lower surface ($z = 0$) are those with wave vectors $\mathbf{k}^{(1)}$, $\mathbf{k}^{(2)}$ and $\mathbf{k}^{(3)}$, because we recall that for a negative group velocity the Poynting vector is opposite to the wave vector. For the same reason waves with wave vectors $\mathbf{k}^{(1r)}$, $\mathbf{k}^{(2r)}$ and $\mathbf{k}^{(3r)}$ are propagating away from the upper surface ($z = L$). We notice here that figs. 2 and 3 have been plotted assuming negligibly small losses, and that in general the wave vectors must be considered complex.

We now consider an incident plane wave of a single frequency for which

$$\mathbf{E}_0(\mathbf{r}, t) = \tilde{\mathbf{E}}_0 \exp\left[i\mathbf{k}^0\mathbf{r} - i\omega t\right], \tag{11}$$

having in mind that the actual "incoming" fields can be written as integrals over $\mathbf{k}^0$ and/or ω. We remark that $\mathbf{k}^0$ and ω are not necessarily linked by the dispersion law in vacuum, because of the presence of an external current due to the oscillating source dipole. Since there is homogeneity in the (x, y)-plane for $z > z_0$ the wave vectors of all the plane waves propagating in vacuum or in the slab must have the same components $k_x \equiv k_x^0$ and $k_y \equiv k_y^0$. Moreover they all oscillate in time at the same frequency ω so that the third component k_z will be determined for each wave by means of the dispersion law as

$$k_z^{(m)} = \pm\sqrt{n_m^2\omega^2/c^2 - k_x^2 - k_y^2}, \tag{12}$$

where $m = \{R, T, 1, 2, 3, 1r, 2r, 3r\}$ denotes one of the plane waves present in our system. The sign of $k_z^{(m)}$ is always chosen in such a way that its imaginary part is positive for waves propagating in the positive z direction and negative for waves propagating in the negative z direction.

For small wave vectors $k^0_{x,y}$ and small losses, we obtain that $k_z^{(m)}$ are nearly real and from relations (10) it follows that in our case we must have

$$\Re(k_z^{(1)}) > 0, \tag{13}$$

$$\Re(k_z^{(2)}) < 0, \tag{14}$$

$$\Re(k_z^{(3)}) < 0. \tag{15}$$

Using the explicit expression of the generalized dielectric constant it can be verified that the above inequalities are always satisfied when the modes (2) and (3) have a negative group velocity.

We now need to compute the amplitudes of 8 waves, by imposing boundary conditions on the slab surfaces. There are two unknown quantities for each transverse wave and one for each longitudinal wave: that makes a total of 14 unknowns, while from the continuity of the tangential components of E and B at the two surfaces we obtain only 8 equations. This is because in our system 3 modes are allowed to propagate inside the slab and we need therefore to specify some Additional Boundary Condition (ABC). The problem of ABCs in molecular crystals has been discussed extensively by Agranovich and Ginzburg [2], who studied the problem from the microscopic point of view. We only mention here that in the case under investigation it is appropriate to use Pekar's boundary conditions [23] and impose that the macroscopic excitonic polarization vanishes at the surface. The excitonic polarization $\mathbf{P}^{\mathrm{ex}}$ can be written as

$$\mathbf{P}^{\mathrm{ex}} = \frac{\tilde{\epsilon}(\omega, \mathbf{k}) - \epsilon_{\mathrm{b}}}{4\pi}\ \mathbf{E}, \tag{16}$$

so that by imposing $\mathbf{P}^{\mathrm{ex}} = 0$ at both surfaces, we obtain the other 6 equations.

Such ABCs allow the calculations of the amplitudes of all the propagating waves. When only one transverse mode is allowed to propagate inside the slab, then it is enough to impose the continuity of the tangential components of the fields. Another possibility is to neglect the longitudinal mode from the calculations; in that case we need only half of the ABCs, and we choose to impose $P_z^{\mathrm{ex}} = 0$. Note that in all the above equations only n^2 has been used.

4. – Numerical calculations

The numerical calculations have been performed as follows. The field created by the oscillating dipole has been decomposed into a sum of plane waves and for each incoming plane wave we solved Maxwell equations with the help of the additional boundary conditions described in previous section. The electric and magnetic fields are finally computed everywhere in space as a sum of the appropriate plane waves.

In order to simplify the calculations, we introduce the nondimensional parameters

$$\omega^* = \omega/\omega_0\,, \tag{17}$$

$$F^* = F/\omega_0^2\,, \tag{18}$$

$$\alpha^* = \alpha/c^2\,, \tag{19}$$

$$\gamma^* = \gamma/\omega_0\,, \tag{20}$$

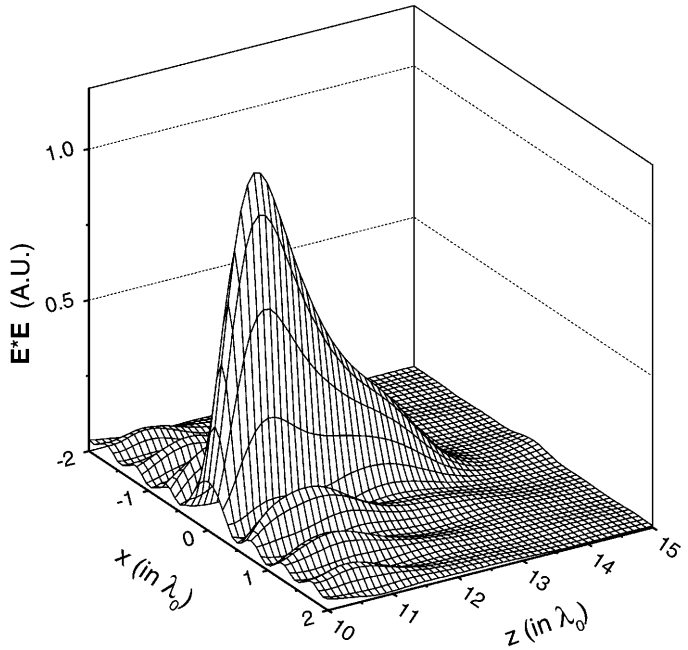

Fig. 4. – Average intensity of the transmitted electric field computed for an oscillating point dipole placed at a distance $d = 0.2\lambda_0$ from a slab of thickness $L = 10\lambda_0$. The maximum intensity is obtained at $z = 10.8\lambda_0$ which can be assumed to be the focusing plane. Other parameters as indicated in the text.

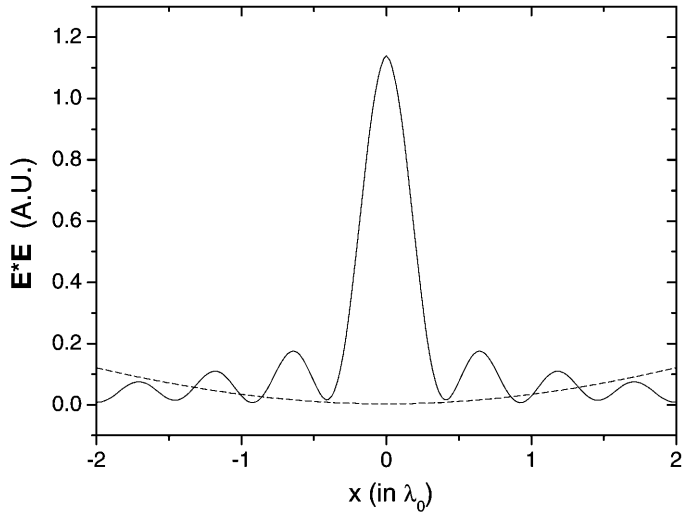

Fig. 5. – Average intensity of the transmitted electric field computed in the presence of the slab (solid line), for the same parameters as in fig. 4. The intensity obtained without the slab ($\times 200$) is also shown for comparison (dashed line).

and the scaled quantity

$$\mathbf{k}^* = \mathbf{k}/k_0\,, \tag{21}$$

where $k_0 = \omega_0/c$ and the corresponding wavelength $\lambda_0 = 2\pi/k_0$ is the main scale length of our problem. The generalized dielectric constant reads

$$\tilde{\epsilon}(\omega^*, \mathbf{k}^*) = \epsilon_\mathrm{b} + \frac{F^*}{1 - \omega^{*2} - i\gamma^*\omega^* + \alpha^* k^{*2}}\,. \tag{22}$$

We recall that in organic crystals excitonic transitions are in the visible range of the spectrum, so that $\hbar\omega_0 \approx 2$ eV corresponding to $\lambda_0 \approx 400$ nm. In order to illustrate what should be possible to observe experimentally, we will consider the following set of parameters:

$$\alpha^* = -0.01, \tag{23}$$

$$F^* = 0.01, \tag{24}$$

$$\epsilon_\mathrm{b} = 1, \tag{25}$$

$$\gamma^* = 10^{-4}, \tag{26}$$

$$\omega^* = 0.98, \tag{27}$$

which serves as a starting point to describe the behavior of real organic crystals. Losses are included in the numerical calculations for every region of space, in order to avoid singular points in the computation of the fields, and in particular we set $\epsilon_0 = 1 + i10^{-8}$ for the vacuum, which is therefore nearly lossless.

We first consider a slab of thickness $L = 10\lambda_0$, delimited by the planes $z = 0$ and $z = 10\lambda_0$, and a dipole located at $\mathbf{r}_0 = (0, 0, -0.2\lambda_0)$, *i.e.* at a distance $d = 0.2\lambda_0$ from the slab. Our goal is to investigate the transmitted field on the opposite side of the slab with respect to the source dipole.

In fig. 4 we show the results of our numerical simulation for the average intensity of the transmitted electric field over a whole oscillation in the region $z > L$. We note that close to the slab a sharp peak appears, which can be interpreted as the real image of the source point dipole produced by the slab. The focusing plane can be identified with the plane $z = 10.8\lambda_0$ where the intensity reaches its maximum and where the best image of the source is obtained. The electric field intensity at the focusing plane is shown in fig. 5 as the solid line and it is compared with the intensity we would measure without the slab. Note how the image obtained in the presence of the slab is predicted to be 3-4 orders of magnitude more intense than the signal without the slab (not to scale in the figure), which displays no peaks. The image has a Full Width at Half Maximum (FWHM) of about 0.30 λ_0 and displays many side peaks, despite the source is assumed to be a delta-function in space. This is because our material is mainly focusing the propagating part of the source, while its evanescent part is only partially amplified. As a matter of fact the propagating part of the fields in vacuum has a minimum spatial wavelength parallel to the slab of $\lambda_r^{\min} = \omega^* \Re[n_0] = 0.98\lambda_0$, which produces a minimum FWHM of about $0.35\lambda_0$ for the observed intensity. We therefore conclude that the slab is able to focus part of the evanescent waves.

If the source is moved away from the slab, then the image is correspondingly shifted toward it, as shown in fig. 6, where the electric field intensity along the symmetry axis is

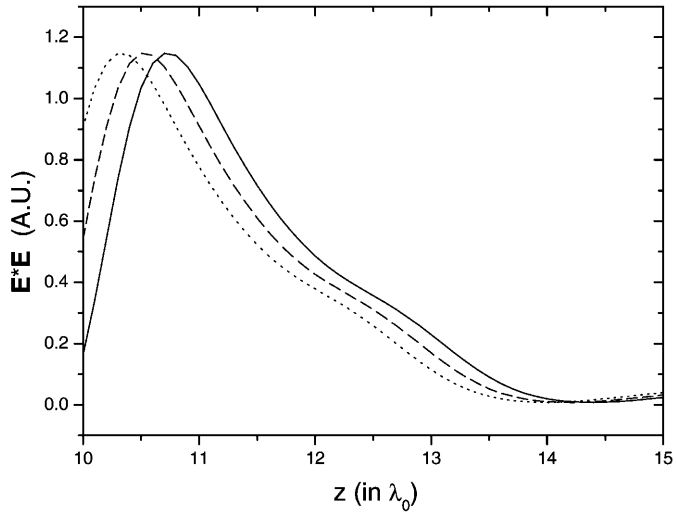

Fig. 6. – Average intensity of the transmitted electric field computed in the presence of the slab for the same parameters as in fig. 4 and different positions of the source dipole: $d = 0.2$ (solid line), 0.4 (dashed line) and 0.6 (dotted line) λ_0.

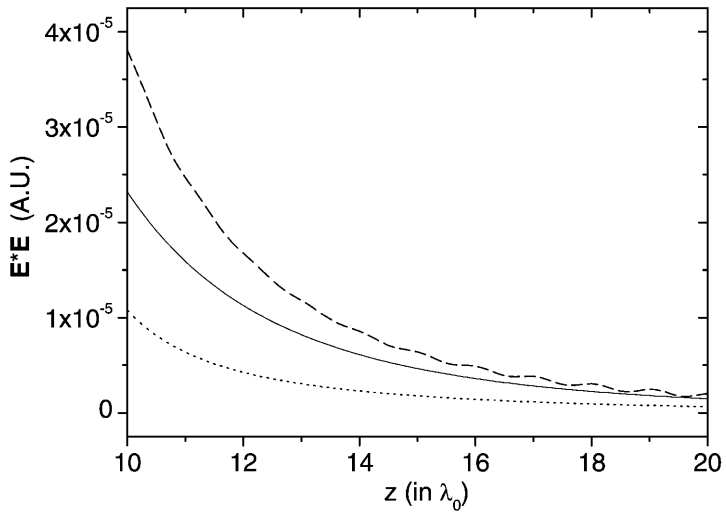

Fig. 7. – Average intensity of the transmitted electric field computed without the slab (solid line), in the presence of a slab with the same parameters as in fig. 4 but considering only the normal transverse mode (dashed line) and in the presence of a slab with parameters given in the text where three right-handed modes where allowed to propagate (dotted line).

plotted. This is in agreement with the fact that the image is due to negative refraction at the slab/air interfaces as shown in fig. 1.

We now want to prove that the above results are indeed due to the left-handed behavior of the additional transverse and longitudinal modes. In order to do so, we plot in fig. 7 the average electric field intensity along z, obtained in three different situations: when no slab is present, when only the normal transverse mode is allowed to propagate inside the slab and when the dispersion curves are similar to the ones in fig. 2a, so that three right-handed modes propagate inside the slab. In this latter case we used $\alpha^* = 0.01$, $\omega^* = 1.02$ and all other parameters as for previous figures. The numerical results reported in fig. 7 show that in all three cases the intensity is much lower than in the presence of the slab and that no peaks appear along z. We also found that in all three cases there was not any peak in the direction parallel to the slab, and that the overall intensity distribution in space was very similar to the one expected for the far field of a dipole in vacuum. We conclude that the image is due to additional waves with negative group velocity.

Some final comment must be made on the importance of the various parameters we used in our calculations. The width of the excitonic resonance γ determines the order of magnitude of the losses inside the slab and its value is fundamental to observe the image. Increasing the value of γ we found that the image becomes less intense until it finally disappears. Another important quantity is the exciton mass which determines the value of α and which is assumed to be negative. When $|\alpha|$ is decreased the negative slope of the dispersion curve is less pronounced and the value of n^2 for the left-handed modes increases. This fact has two negative consequences: first the transmitted intensity, specially that part due to the left-handed modes, decreases and second the slab must be thicker and thicker to properly focus the image, which is therefore very weak. The other parameters are not as important as the above-mentioned ones, and they mainly determine the details of the dispersion curves.

5. – Conclusions

We have demonstrated that organic crystals with appropriate spatial dispersion exhibit negative refraction at optical frequencies close to the excitonic transitions. This is possible due to the appearance of additional waves with negative group velocity inside the crystal when the exciton mass is negative. We studied in detail the case of a plane slab which acts as a lens, focusing the light coming from a point source dipole, and we used appropriate parameters to show the main features of the resulting image. Real crystals have less favorable characteristics, but we believe that it should be possible to observe experimentally the formation of an image in the near field.

REFERENCES

[1] Veselago V. G., *Usp. Fiz. Nauk*, **92** (1967) 517; *Sov. Phys. Usp.*, **10** (1968) 509.
[2] Agranovich V. M. and Ginzburg V. L., *Crystal Optics with Spatial Dispersion, and Excitons* (Springer, Berlin) 1984.
[3] Smith D. R. and Kroll N., *Phys. Rev. Lett.*, **85** (2000) 2933.
[4] Shelby R. A., Smith D. R. and Schultz S., *Science*, **292** (2001) 77.
[5] Pendry J. B., *Phys. Rev. Lett.*, **85** (2000) 3966.
[6] Pendry J. B. and Ramakrishna S. A., *J. Phys. Condens. Matter*, **14** (2002) 1.
[7] Pendry J. B., *Opt. Express*, **11** (2003) 755.

[8] Smith D. R., Shurig D. and Pendry J. B., *Appl. Phys. Lett.*, **81** (2002) 2713.
[9] Parazzoli C. G., Greegor R. B., Li K., Koltenbah B. E. C. and Tanielian M., *Phys. Rev. Lett.*, **90** (2003) 107401.
[10] Houck A. A., Brock J. B. and Chuang I. L., *Phys. Rev. Lett.*, **90** (2003) 137401.
[11] Kosaka H., Kawashima T., Tomita A., Notomi M., Tamamura T., Sato T. and Kawakami S., *Phys. Rev. B*, **58** (1998) R10096.
[12] Notomi M., *Phys. Rev. B*, **62** (2000) 10696.
[13] Ochiai T. and Sanchez-Dehesa J., *Phys. Rev. B*, **64** (2001) 245113.
[14] Luo C., Johnson S. G., Joannopoulos J. D. and Pendry J. B., *Phys. Rev. B*, **65** (2002) 201104.
[15] Foteinopoulou S. , Economou E. N. and Soukoulis C. M., *Phys. Rev. Lett.*, **90** (2003) 107402.
[16] Cubukcu E., Aydin K., Ozbay E., Foteinopolou S. and Soukoulis C. M., *Phys. Rev. Lett.*, **91** (2003) 207401.
[17] Lu W. T., Sokoloff J. B. and Sridhar S., *Phys. Rev. E*, **69** (2003) 026604.
[18] Smith D. R. and Schurig D., *Phys. Rev. Lett.*, **90** (2003) 77405.
[19] Pacheco Jr. J., Grzegorczyk T. M., Wu B.-I., Zhang Y. and Kong J. A., *Phys. Rev. Lett.*, **89** (2002) 257401.
[20] Yong Zhang, Fluegel B. and Mascarenhas A., *Phys. Rev. Lett.*, **91** (2003) 157404.
[21] Agranovich V. M., Shen Y. R., Baughman R. H., and Zakhidov A. A., *Phys. Rev. B*, **69** (2004) 165112; *J. Lumin.*, **110** (2004) 167.
[22] Landau L. D. and Lifshits E. L., *Electrodynamics of Continuous Media*, 2nd ed. (Pergamon Press, New York) 1960, Chapt. IX.
[23] Pekar S. I., *Sov. Phys. JETP*, **6** (1958) 785.